Direct Torque Control for Permanent Magnet Synchronous Motor Based on NARMA-L2 controller

Dr. Abdulrahim T. Humod
Electrical Engineering Department, University of Technology / Baghdad.
Dr. Ali H. Almukhtar
Electrical Engineering Department, University of Technology / Baghdad.
Huda B. Ahmed
Electrical Engineering Department, University of Technology / Baghdad.

Received on:16/9/2015 & Accepted on:17/١٢/2015

ABSTRACT

This paper investigates the improvement of the speed and torque dynamic responses of three phase Permanent Magnet Synchronous Motor (PMSM) using Direct Torque Control (DTC) technique. Different torques are applied to PMSM at different speeds during operation to ensure the robustness of the controller for wide torque variations. Optimal PI controller is used to modify the response of DTC. The optimal gains of PI controller are tuned by Particle Swarm Optimization (PSO) technique. Neural Network controller is called the Nonlinear Autoregressive-Moving Average (NARMA-L2) which is trained based on optimal PI controller (PI-PSO) data. The results show the superiority performance of using NARMA-L2 controller on PI-PSO controller for different speeds and load change. The overall simulation and design of the scheme are implemented Using MATLAB/Simulink program.

Keywords: Permanent Magnet Synchronous Motor (PMSM), Direct Torque Control (DTC), Proportional- Integral (PI), Particle Swarm Optimization (PSO) and NARMA-L2 controller.

السيطرة المباشرة على العزم للمحرك التزامني ذو المغناطيس الدائم باستخدام تقنية NARMA-L2)

الخلاصة

تم في هذا البحث دراسة تحسين استجابة السرعة والعزم الديناميكية للمحرك ثلاثي الاطوار التزامني ذو المغناطيس الدائم (PMSM) باستخدام تقنية السيطرة المباشرة على العزم (DTC). تم تجهيز المحرك التزامني ذو المغناطيس الدائم بعزوم مختلفة خلال سرع مختلفة لضمان الحصول على مسيطر أكثر متانة لمتغيرات الحمل والسرعة. استخدم المسيطر التناسبي-التكاملي (PI) المثالي لتعديل استجابة ال (DTC). المتغيرات (gains) المثالية للمسيطر (PI) تم ضبطها باستخدام تقنية أفضلية الحشد الجزيئي (PSO). قد درب المسيطر المعتمد على الشبكات العصبية الاصطناعية (NARMA-L2)على النتائج التي تم الحصول عليها من المسيطر (PI-PSO). اظهرت النتائج اداءاً متفوقاً عند استخدام المسيطر (NARMA-L2) على المسيطر (PI-PSO) لسرعات متغيرة وبتغير الحمل. تم تنفيذ المحاكاة الشاملة وتصميم المخطط باستخدام برنامج MATLAB/ SIMULINK

INTRODUCTION

https://doi.org/10.30684/etj.34.3A.4
2412-0758/University of Technology-Iraq, Baghdad, Iraq

In the middle of 1980s, Takahachi and Noguchi first projected Direct Torque Control (DTC) method for low and medium power applications of induction machines. In addition, this model can also be applied to synchronous machines and DTC has performed in the late 1990s [1]. The inverter state is directly controlled by DTC which depends on the errors between the reference and estimated values of torque and flux. To keep torque and flux within the limits of two hysteresis bands, DTC selects one of six voltage vectors produced by a Voltage Source Inverter (VSI) [2].

Different techniques of intelligent control have been realistic to DTC used for EV in estimation and control to get high performance in these drives such as Zhengqiang (2005) [**3]** proposed an intelligent controller for a PMSM in a Hybrid Electric Vehicle (HEV) application. Improved Particle Swarm Optimization (IPSO) method is used to improve three proportional parameters of Fuzzy Logical Controller (FLC) online increasing the robustness of overall system. Jalal (2007) [4] proposed a simulation of Artificial Neural Networks (ANNs) for training and estimation of electromagnetic torque, flux and flux angle, based on the stator voltages and currents. Genetic Algorithm (GA) is suggested for stator resistance optimization, which can improve the DTC performance. Singh (2008) [5] used Neural Network (NN) on DTC scheme of Interior Permanent Magnet Synchronous Motor (IPMSM) for EV. Bossoufi (2011) [6] suggested an intelligent artificial technique for improvement of DTC of PMSM such as ANN, applied in switching select voltage vector and estimator flux and torque. This intelligent technique was used to replace the conventional comparators and the switching table in order to reduce torque ripple. Hussen (2012) [7] proposed high performance FOC of PMSM. The main objective is to improve the performance of PMSM during different load and speed condition. Two types of controllers are used; the first controller is the Proportional-Integral (PI) based on PSO technique. The second controller is Fuzzy-PI with scaling factor (gain) tuned by PSO technique. The results show the improvement in the performance of Fuzzy-PI using PSO technique on conventional PI and PI-PSO. Humod [2013] [8] proposed DTC control technique to propose Direct Torque Control (DTC). Particle Swarm Optimization (PSO) technique is used for optimal gains tuning of PI. The result show the improvement in the speed response of DTC, in terms of reducing steady state error, ripple reduction in the torque and speed responses. Neurofuzzy(ANFIS) controller is used to improve the performance of PI-PSO controller. In this work neural network (NARMA-L2) to improve the performance of DTC.

Mathematical Model of PMSM

To derive of two phase (***d, q***) PMSM mathematical model, the next assumptions are made [9]:

1. Sinusoidal MMFallocation is created by stator winding. Space harmonics in air gaps are ignored
2. Reluctance of air gap has a constant element in addition to a sinusoidally fluctuating element
3. Consideration of three phase source voltage is balanced
4. Ignoring saturation
5. Sinusoidal back EMF
6. ignoring both eddy currents and hysteresis losses

In the rotor (***d, q)*** reference frame, the scalar procedure of voltage equations are as follows [10]:

$$\boldsymbol{V\_d = R\_s\, i\_(d) + d/dt\,(\psi\_(d)) - \omega\_e\, \psi\_q} \quad \ldots (1)$$

$$\boldsymbol{V\_q = R\_s\, i\_(q) + d/dt\,(\psi\_(q)) + \omega\_e\, \psi\_d} \quad \ldots (2)$$

Where,

$\boldsymbol{[V]\_d}$ and $\boldsymbol{V\_q}$ are the (d , q) axis voltages in the rotor reference frame (v);

$\boldsymbol{i\_d}$ and $\boldsymbol{[i]\_q}$ are the (d , q) axis currents in the rotor reference frame (Amp.);

$\boldsymbol{R\_s}$ is the stator phase resistance[Ω], where ($R\_d = R\_q \ \ \llbracket = R \rrbracket \_s$);
$\boldsymbol{\omega\_e}$ is the electrical rotor speed [rad/s];
$\boldsymbol{\psi\_(d}$) and $\boldsymbol{\psi_q}$are the (d, q) axis flux linkage in the rotor reference frame (Wb);
The flux linkage equations are:

$$\boldsymbol{\psi\_(d =) \ L\_d \ i\_d + \psi\_pm} \quad \ldots (3)$$

$$\boldsymbol{\psi\_(q =) \ L\_q \ i\_q} \quad \ldots (4)$$

Where,
$\boldsymbol{L\_d}$ and $\boldsymbol{L\_q}$ are the (d , q) axis inductances in the rotor reference frame (***H***);
$\boldsymbol{\psi\_pm}$ is the flux through the stator due to the permanent magnet (Wb).
By substituting the flux equations (3) and (4) in the voltages equations (1) and (2) the compact form of the voltage is obtained as shown in equations (5) and (6).

$$\boldsymbol{V\_d = (R\_s \ + L\_(d \ ) \ d/dt) \ i\_d - \omega\_e \ L\_q \ i\_q} \quad \ldots (5)$$

$$\boldsymbol{V\_q = (R\_s \ + L\_(q \ ) \ d/dt) \ i\_q + \omega\_e \ L\_d \ i\_d + \omega\_e \ \psi\_pm} \quad \ldots (6)$$

Similarly, the PMSM stator voltages equation can be stated as follows [1]:

$$\begin{bmatrix} V_{sd} \\ V_{sq} \end{bmatrix} = \begin{bmatrix} R_s + L_d \frac{d}{dt} & -\omega_e L_q \\ \omega_e L_d & R_s + L_q \frac{d}{dt} \end{bmatrix} \begin{bmatrix} i_{sd} \\ i_{sq} \end{bmatrix} + \begin{bmatrix} 0 \\ \omega_e \psi_{pm} \end{bmatrix} \quad \ldots (7)$$

And the stator flux linkage can be also expressed in matrix form as:

$$\begin{bmatrix} \Psi_{sd} \\ \Psi_{sq} \end{bmatrix} = \begin{bmatrix} L_d & 0 \\ 0 & L_q \end{bmatrix} \begin{bmatrix} i_{sd} \\ i_{sq} \end{bmatrix} + \begin{bmatrix} \psi_{pm} \\ 0 \end{bmatrix} \quad \ldots (8)$$

Instantaneous power in ***(a-b-c)*** reference system is stated as [7]:

$$\boldsymbol{P\_(in, abc =) \ \llbracket v\_a \ i \rrbracket \_a + \ \llbracket v\_b \ i \rrbracket \_b + \ \llbracket v\_c \ i \rrbracket \_c} \quad \ldots (9)$$

After the stator phase magnitudes are converted to the rotor ***(d, q)*** reference frame, the following equation can be stated:

$$\boldsymbol{P\_(in, dq) = 3/2 \ (\ \llbracket v\_q \ i \rrbracket \_q + \ \llbracket v\_d \ i \rrbracket \_d \ ) + 3 \ \llbracket v\_0 \ i \rrbracket \_0} \quad \ldots (10)$$

Zero sequence is neglected then inserting equations (1) and (2) into (10), yields the following power equation as:

$$\boldsymbol{P\_(in, dq) = 3/2 \ (R\_s \ i\_d\text{\^{}2 + R\_s \ i\_q\text{\^{}2 }) + 3/2 \ (i\_d \ (d\psi\_d)/dt + i\_q \ (d\psi\_q)/dt) + 3/2 \ \omega\_e \ (\psi\_d \ i\_q - \psi\_q \ i\_d \ )} \quad \ldots (11)$$

The mechanical angular frequency can be expressed as $\boldsymbol{\llbracket (\omega \rrbracket \_e = \ p/2 \ \omega\_m}$. Assuming steady state, electromagnetic power $\boldsymbol{P_e}$ can be stated as [7]:

$$\boldsymbol{P\_e = \omega\_m \ (3/2)(p/2)(\psi\_d \ i\_q - \psi\_q \ i\_d \ )} \quad \ldots (12)$$

Divide the power by rotational speed $\boldsymbol{\omega\_m}$ to get the motors electromagnetic torque $\boldsymbol{T\_e}$ as follows [7]:

$$\boldsymbol{T\_e = (3/2)(p/2)(\psi\_d \ i\_q - \psi\_q \ i\_d \ )} \quad \ldots (13)$$

Moreover, replace the flux linkages $\boldsymbol{\psi\_d}$ and$\boldsymbol{\psi_q}$ with equations (2) and (3), the torque equation is obtained:

$$T\_e = (3/2)(P/2)(\psi\_pm\, i\_q + (L\_d - L\_q)\, i\_q\, i\_d \quad \ldots (14)$$

Considering a non-salient rotor (SPMSM), where the inductances equal **(L_d = L_q)**, the final expression of the electromagnetic torque is [10]:

$$T\_e = (3/2)(p/2)(\psi\_pm\, i\_q) \quad \ldots (15)$$

This result is quite interesting. It shows that the only component involved in torque production in a PMSM without saliency is the q axis current.

The expression of the mechanical equation is [10]:

$$T\_e = T\_L + T\_df + B\omega\_m + J\,(d\omega\_m)/d\_t \quad \ldots (16)$$

However, ignoring the dry friction torque, the equation of motion is stated as [3]:

$$[J\,(d\omega\_m)/d\_t\ = T]\_e - T\_L - B\omega\_m \quad \ldots (17)$$

The rotor mechanical speed can be derived from equation (17) as follows:

$$\omega\_m = \int ((T\_e - T\_L - B\omega\_m)/J)dt \quad \ldots (18)$$

Figure (1)shows the dynamics equivalent circuit of the PMSM based on equations (1), (2), (3) & (4).

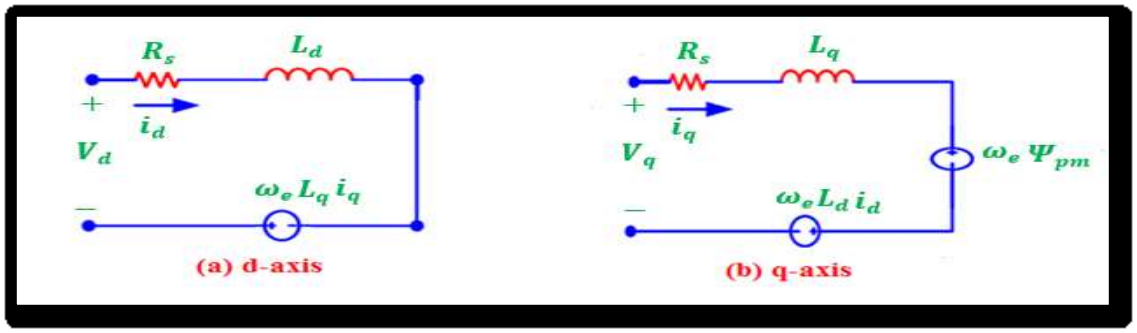

Figure (1): PMSM equivalent circuit.

Direct Torque Control

Figure (2) shows the general block diagram of the DTC control strategy.

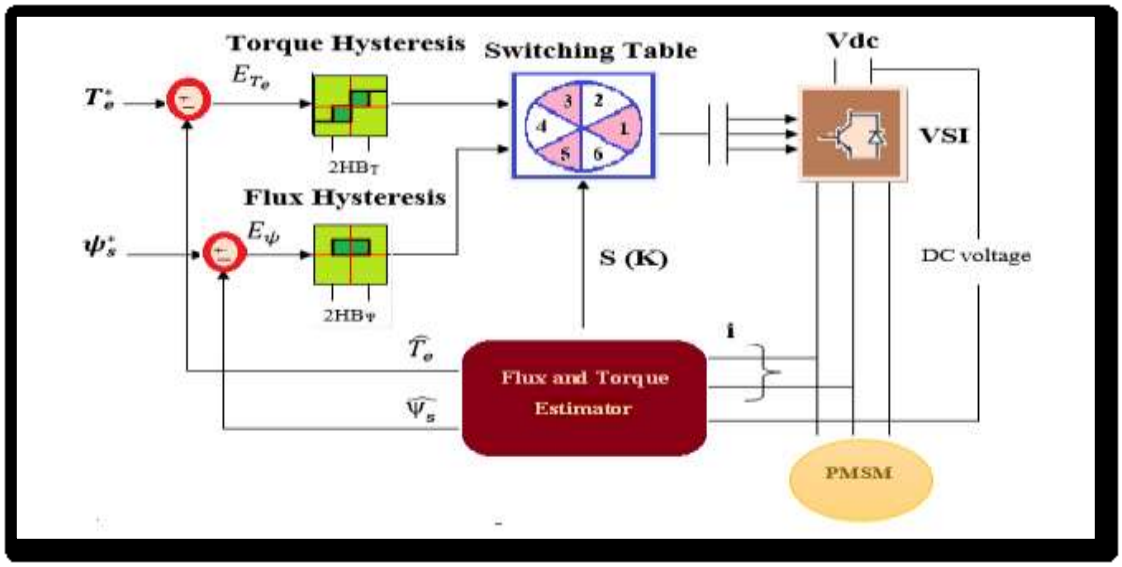

Figure (2): Classical direct torque control block diagram.

The estimator equations for estimated stator flux ($(\psi\_s)\hat{}$), stator flux position ($(\theta\_s)\hat{}$) and estimated torque developed ($(T\_e)\hat{}$) can be expressed as [11] :

$$(\psi\_s)\hat{} = \sqrt{(\ [\![\psi\_qs]\!]\ ^2 + \ [\![\psi\_ds]\!]\ ^2)} \quad \ldots (19)$$

$$(\theta\_s)\hat{} = \ [\![\tan]\!]^{(-1)}\ ([\![\psi\_qs/\psi\_ds]\!]) \quad \ldots (20)$$

$$(T\_e)\hat{} = (3/4)P\ (\psi\_ds\ i\_qs - \psi\_qs\ i\_ds) \quad \ldots (21)$$

Particle Swarm Optimization [7]

To obtain best values for deriving PI controller, PSO procedure is operated. Particles are the possible solutions, which represent the code for fish inside fish schools or bird inside bird flocks. Throughout multidimensional space, these particles are prepared randomly and fly. During the flight and based on knowledge possession of the whole inhabitants, particles renew their position and velocity. The renewing technique will steer the swarm of particle to transfer for the direction of state with superior value of fitness. Lastly, all particles are collected round the best fitness value point.

Based on the following equations, the particles are renewed:

$$[\![v(k+1)]\!]\_(i,j) = [\![w.v(k)]\!]\_(i,j) + c\_1\ r\_1\ (gbest - [\![x(k)]\!]\_(i,j)) + c\_2\ r\_2\ (\ [\![pbest]\!]\_j - [\![x(k)]\!]\_(i,j)) \quad \ldots (22)$$

$$[\![x(k+1)]\!]\_(i,j) = [\![x(k)]\!]\_(i,j) + [\![v(k)]\!]\_(i,j \quad \ldots (23)$$

In the *gbest* mode, the top point found using whichever member of the entire inhabitants influences the path for all particles' search. The best particle attracts every particle to it where its performances are like attractor. Finally, all particles will converge to the best particle position. Through some smaller number of close members of the inhabitant collection, the *pbest* mode allows each individual to be influenced. PSO algorithm is characterized as a simple concept, flexible, easy

to implement high quality solution within a shorter calculation time and has a stable convergence characteristic relative to optimization method like.
The Integral Time Square Error (ITSE) time domain criterion is used as a "Fitness Function (FF)" to estimate the parameters of PI Controller.

NARMA-L2 Control

Narendra and Mukhopadhayay in (1997) proposed the NARMA-L2 model. It can be used to model the plant previously cited, using two distinct neural networks. One net implements a controller and another simulates a model of the plant. The NARMA-L2 uses a nonlinear identification tool. The neurocontroller is referred to by two different names: feedback linearization control and Nonlinear Auto-regressive Moving Average (NARMA). When the plant model has a particular formula (companion formula), the nourocontroller is mentioned to as feedback linearization. It is mentioned as NARMA controller when the same formula can estimate the plant model. To convert the system from nonlinear dynamics into linear dynamics by canceling the nonlinearities, it is the objective of NARMA[12].

Identification of the NARMA-L2 Model

System Identification means inferring a neural network model of the process to be controlled from a set of input-output data collected from the process, i.e. training a neural network to represent the forward dynamics of the system. A standard model structure used to represent general discrete time nonlinear systems is NARMA model [13].
Firstly, selecting a model structure to work. NARMA controller is used to represent common discrete time nonlinear systems where its formula is described as:

$$y(k+d) = N[y(k),y(k-1),\ldots,y(k-n+1),u(k),u(k-1),\ldots,u(k-n+1)] \quad \ldots (25)$$

The system input and output are [$u(k)$, $y(k)$] consequently. To estimate the nonlinear function N, an NN is trained for the identification segment. This is the identification procedure for the NN Predictive Controller. To make the output system follow some reference trajectory by developing a nonlinear control described in the following formula:

$$y(k+d) = yr(k+d) \quad \ldots (26)$$

$$u(k) = G[y(k),y(k-1),\ldots,y(k-n+1),yr(k+d),u(k-1),\ldots,u(k-m+1)] \quad \ldots (27)$$

The problem with using this controller is training neural network to minimize mean square error, it needs to use dynamic back propagation which is quite slow [12]. Using approximate models to characterize the system is the best solution. NARMA-L2 approximate model is:

$$\hat{y}(k+d) = f[y(k),y(k-1),\ldots,y(k-n+1),u(k-1),\ldots,u(k-m+1)] + g[y(k),y(k-1),\ldots,y(k-n+1),u(k-1),\ldots,u(k-m+1)]u(k) \quad \ldots (28)$$

where the next controller input is not contained inside the nonlinearity. The advantage of this form is that controlled input makes the system output follow the reference equation (28). The resulting controller would have the form:

$$u\_((k)) = (y\_r(k+d) - f[y(k),y(k-1),..,y(k-n+k),u(k-1),..u(k-m+1))/(g[y(k),y(k-1),\ldots y(k-n+1),u(k-1),\ldots u(k-n+1)) \quad \ldots (29)$$

Using this equation directly can cause realization problems, because one must determine the control input based on the output at the same time, i.e.:

$$y(k+d) = f[y(k),y(k-1),..,y(k-n+1),u(k),u(k-1),\ldots,u(k-n+1)] + g[y(k),\ldots,y(k-n+1),u(k),\ldots,u(k-n+1)]u(k+1) \quad \ldots (30)$$

The previously identified NARMA-L2 plant model can implement this controller as presented in Figure (3).

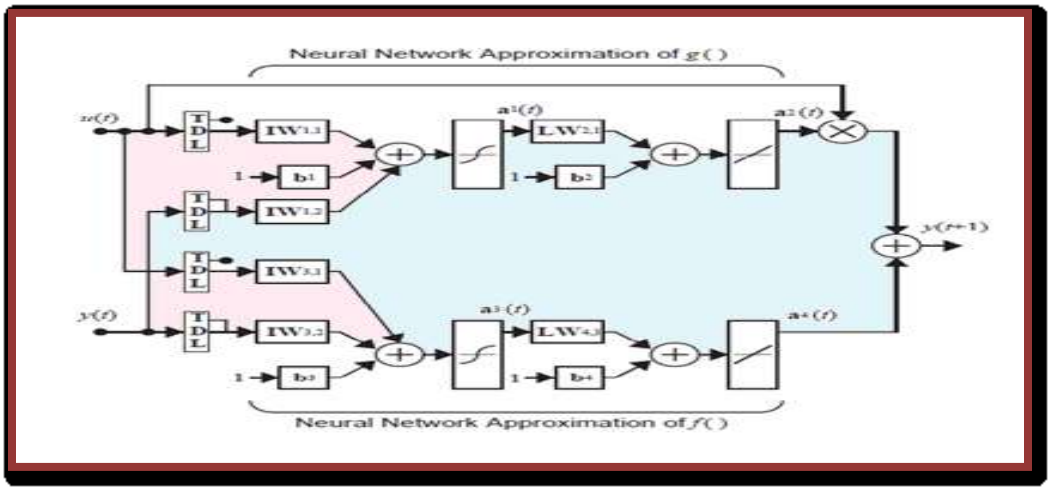

Figure (3): The structure of NN representation.

NARMA-L2 Controller

The advantage of the NARMA-L2 form is that you can solve for the control input that causes the system output to follow a reference signal as shown in Figure (4) [12].

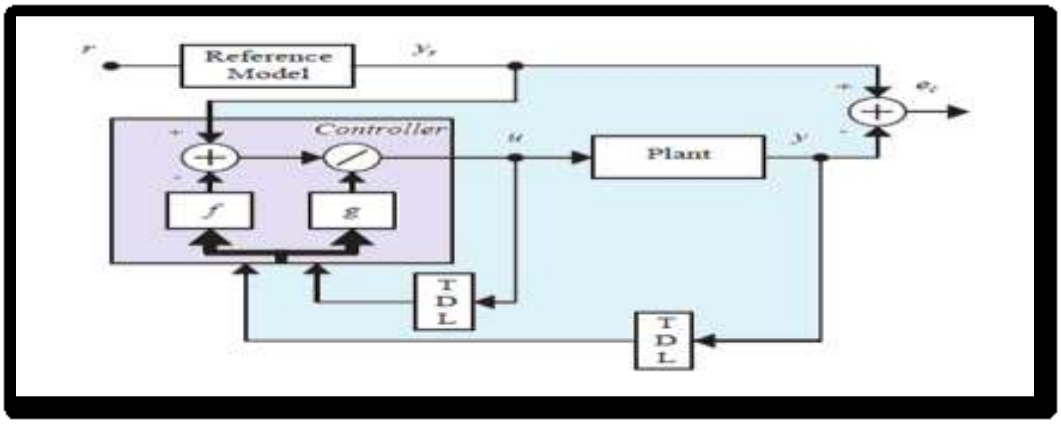

Figure (4): Block diagram of NARMA-L2 controller.

Simulation and Results

The values of the electrical design parameters for three-phase PMSM used in the simulation are shown in the appendix A and the look up table that used for optimum switching states is shown in appendix B. Figure (5) shows the MATLAB/Simulink circuit of the conventional DTC.

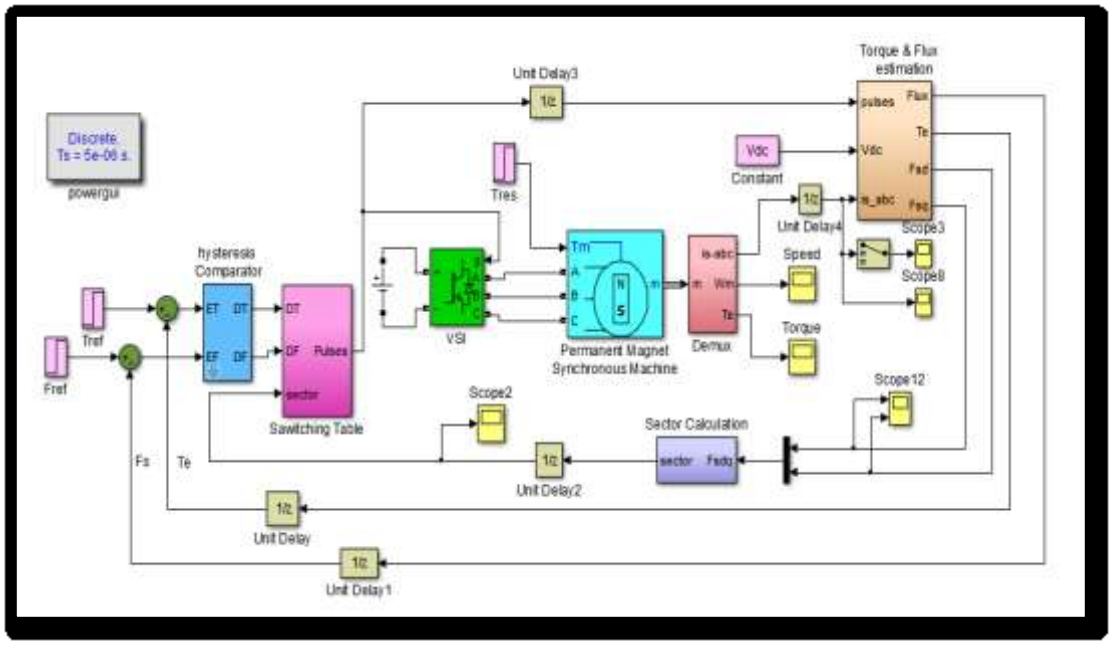

Figure (5): Conventional DTC MATLAB/Simulink circuit

The DTC with PI-PSO controller MATLAB/Simulink circuit is shown in Figure (6).

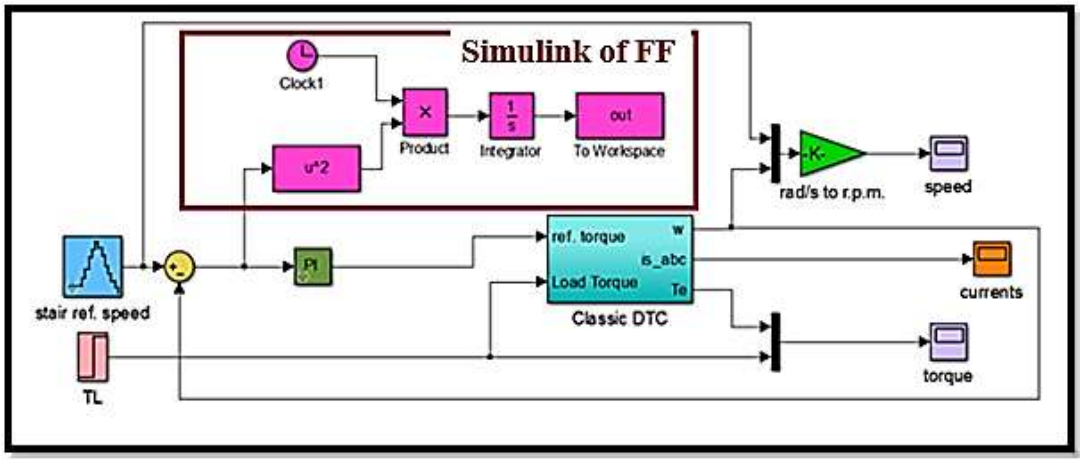

Figure (6): DTC with PI-PSO controller MATLAB/SIMULINK circuit.

The optimal PI-controller gains tuned by PSO method are 〖(K〗_p = 5.378 and K_i = 5.988). The flow chart of PSO gains tuning algorithm show in Figure (7).

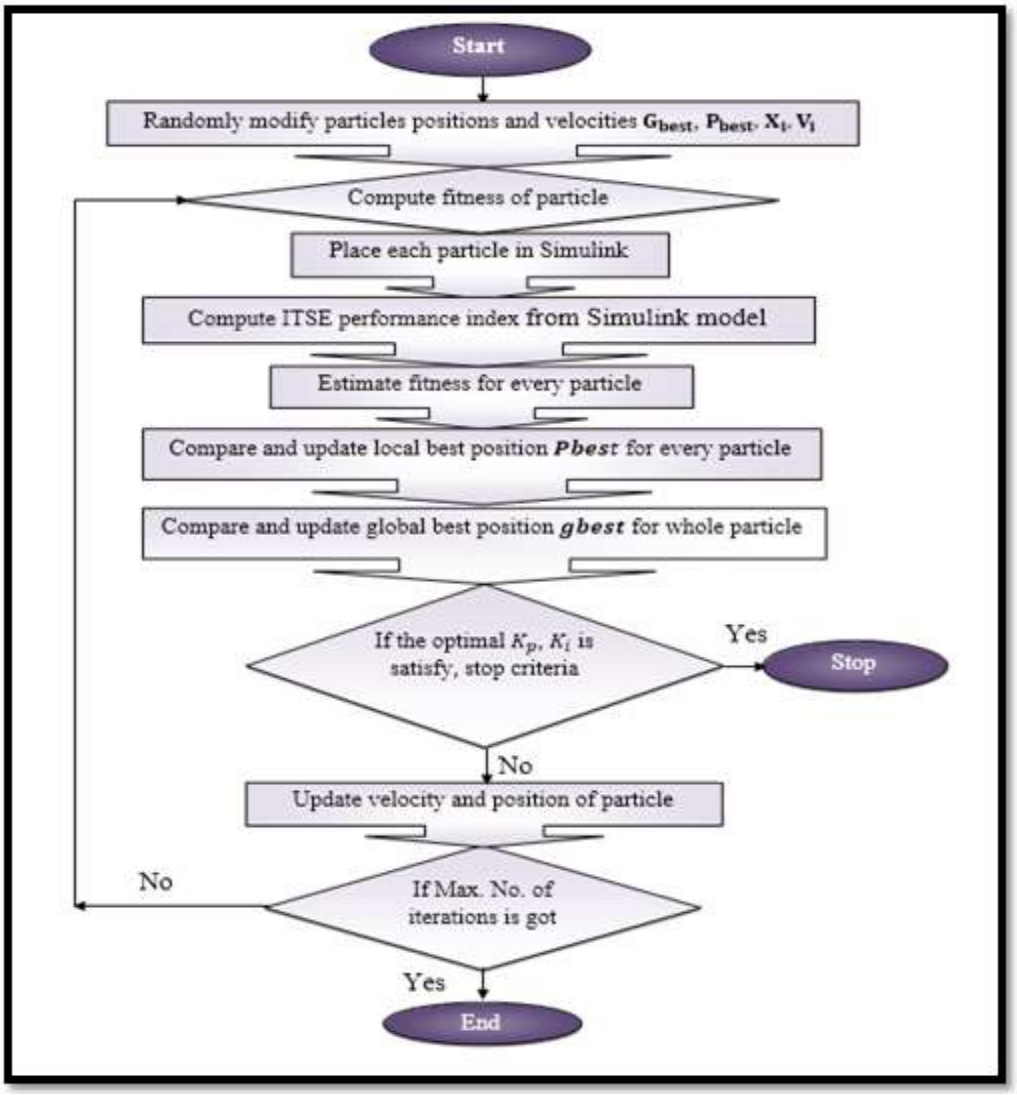

Figure (7): Flowchart of PSO gains tuning algorithm.

The torque is transformed from the no load condition four times, the changes are (50, 70, 90, 110) N.m. Figures (8), (9), (10), (11) and (12) shows the speed and torque responses at different load conditions with the same changes of speed.

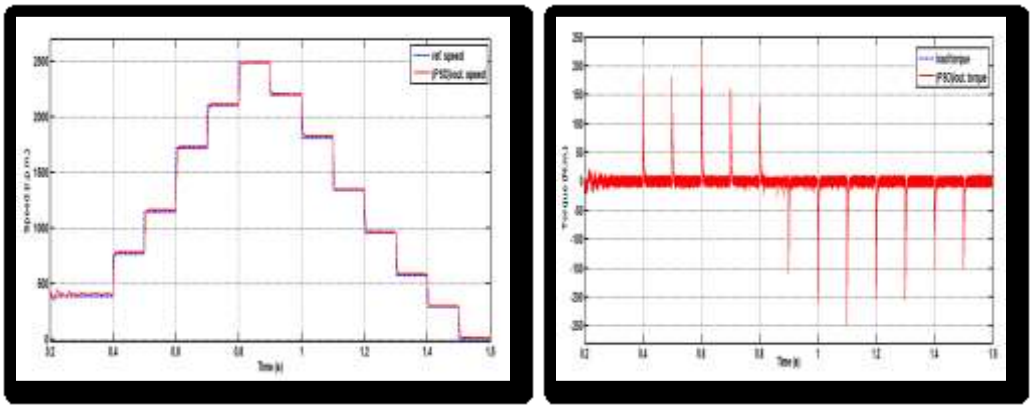

(A) (B)

Figure (8): PI-PSO controller at no load (A) Speed response, (B) Torque response

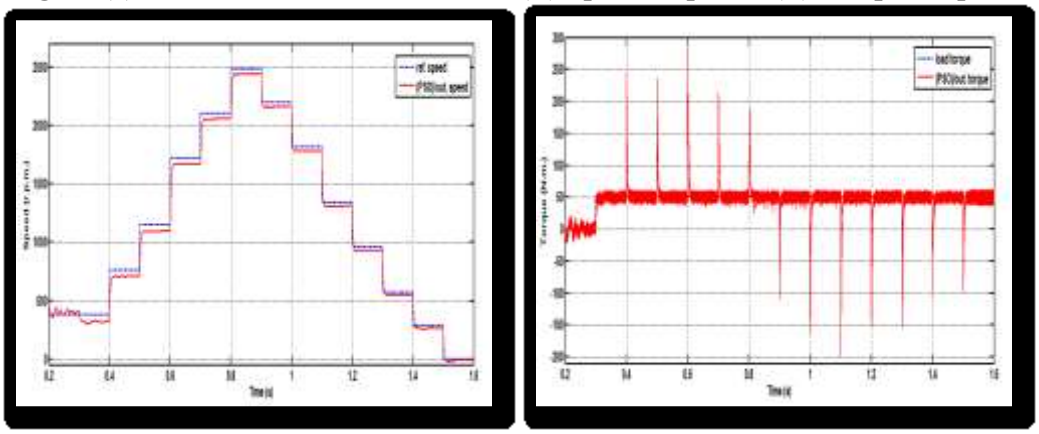

(A) (B)

Figure (9): PI-PSO controller at (50 N.m.) load torque (A) Speed response, (B) Torque response

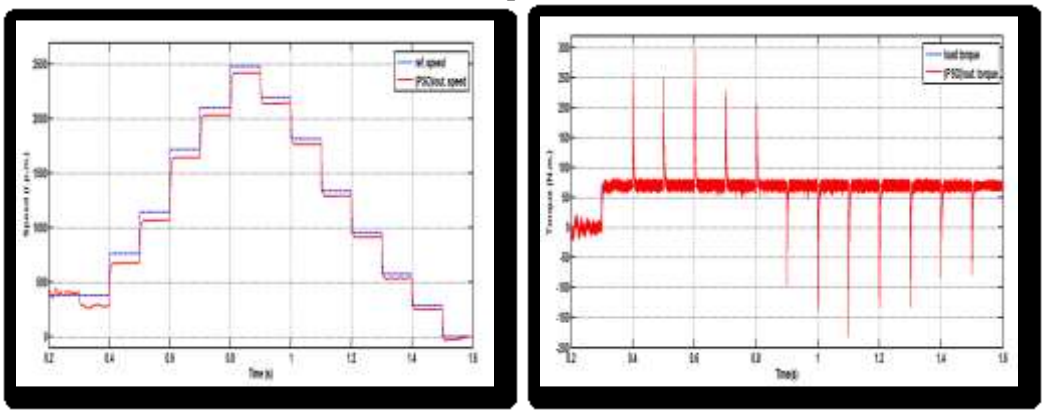

(A) (B)

Figure (10): PI-PSO controller at (70 N.m.) load torque (A) Speed response, (B) Torque response

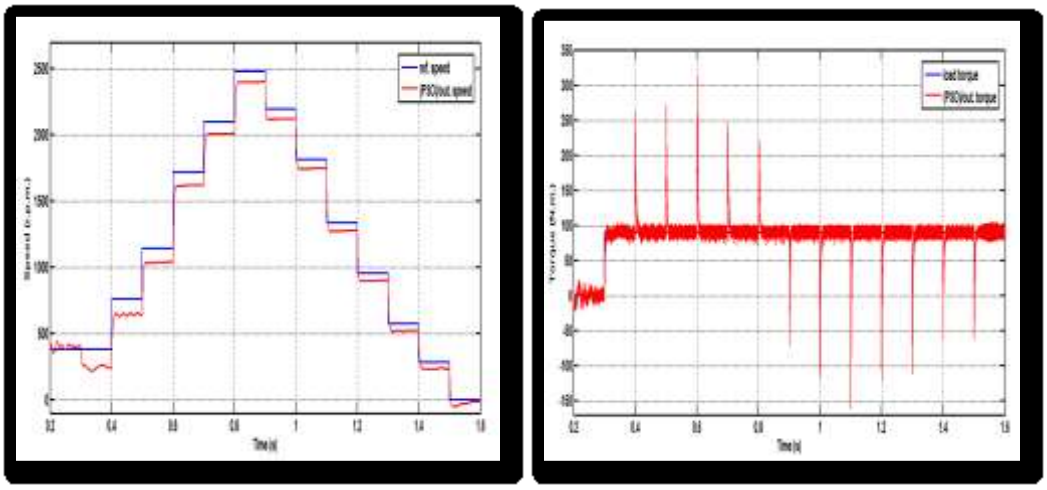

(A) (B)

Figure (11): PI-PSO controller at (90 N.m.) load torque (A) Speed response, (B) Torque response

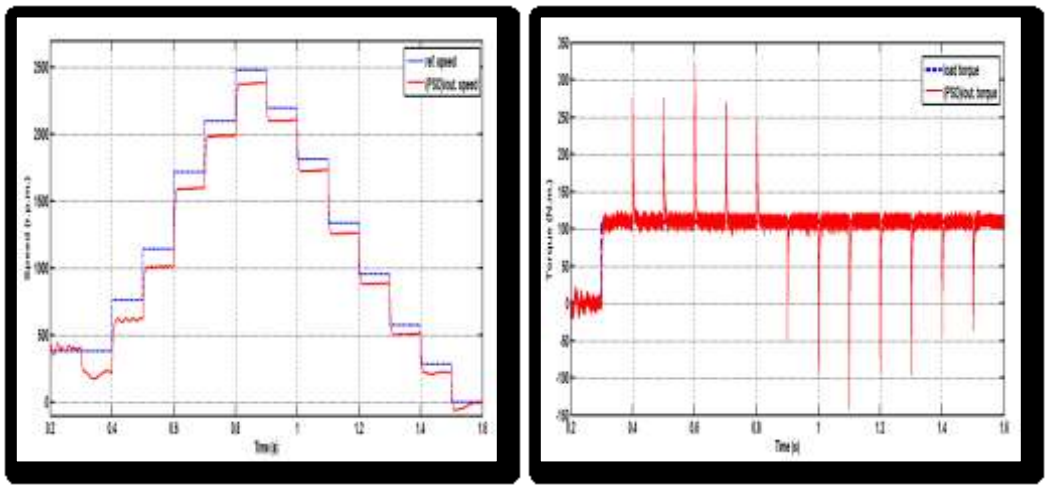

(A) (B)

Figure (12): PI-PSO controller at (110 N.m.) load torque (A) Speed response, (B) Torque response.

The system of PMSM with DTC using NARMA-L2 controller is represented by block diagram shown in Figure (13).

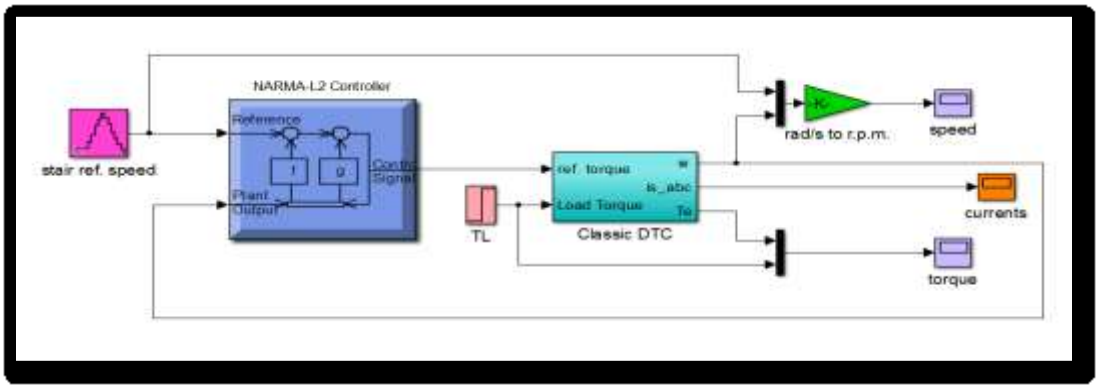

Figure (13): DTC with NARMA-L2 controller MATLAB/Simulink circuit.

The flow chart of NARMA-L2 simulation show in Figure (14).

Figure (14): Flow chart of running NARMA-L2 program.

Speed and torque responses of PMSM for NARMA-L2 controller at different loads are shown in Figures (15), (16), (17), (18) and (19).

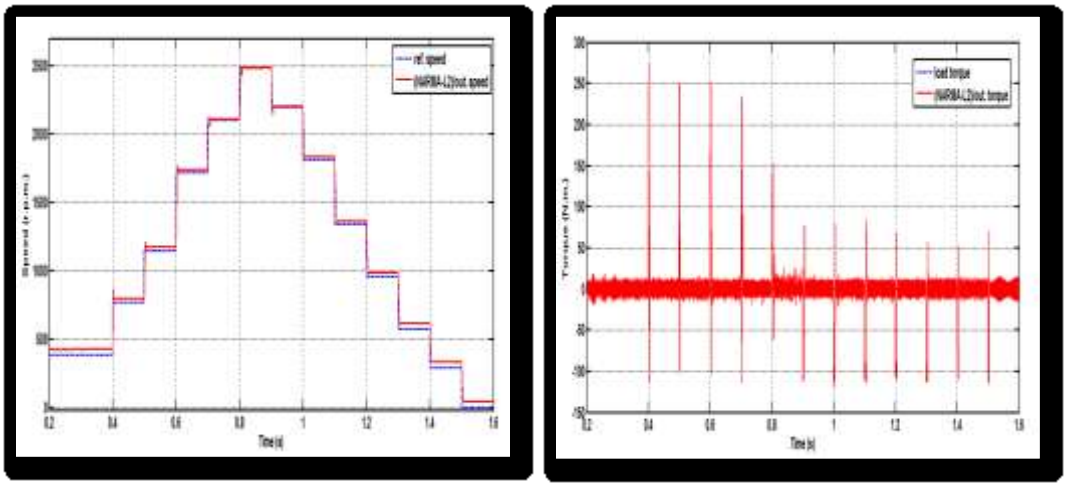

(A) **(B)**

Figure (15): NARMA-L2 controller at no load (A) Speed response, (B) Torque response.

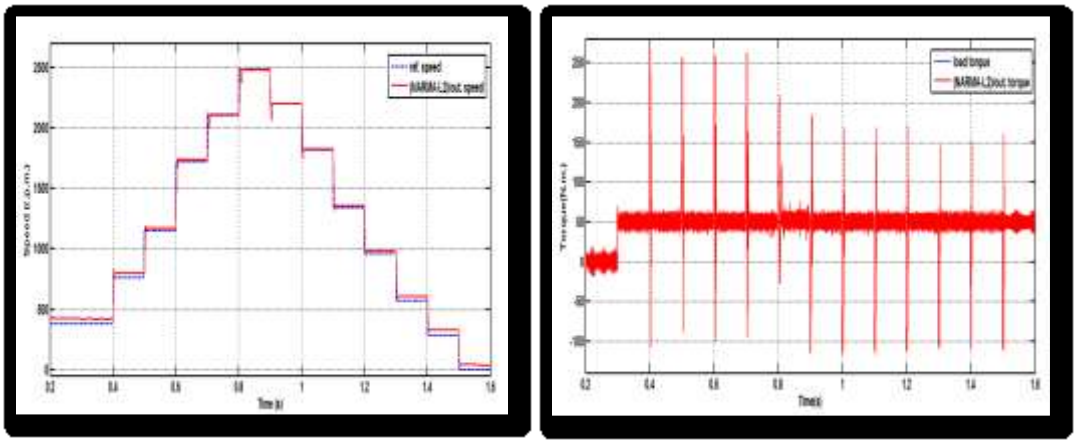

(A) **(B)**

Figure (16): NARMA-L2 controller at (50 N.m.) load torque (A) Speed response, (B) Torque response.

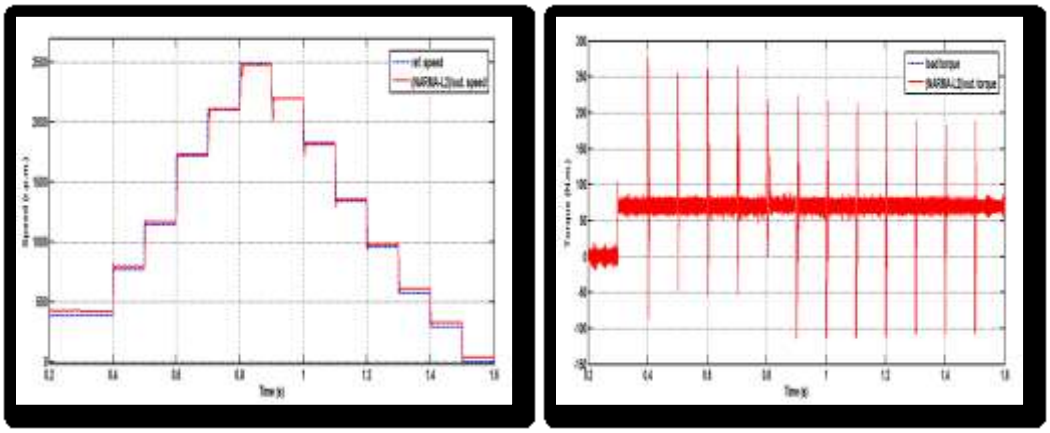

(A) **(B)**

Figure (17): NARMA-L2 controller at (70 N.m.) load torque (A) speed response, (B) Torque response.

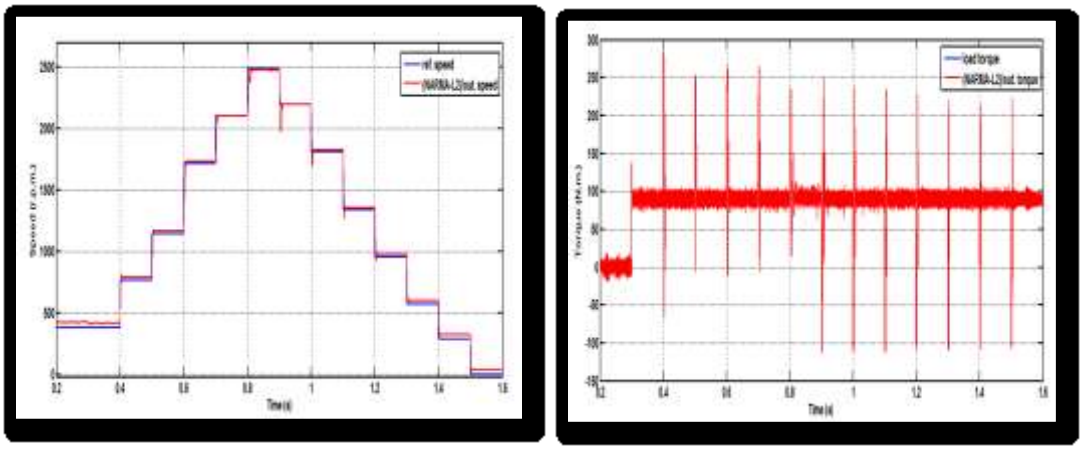

(A) **(B)**

Figure (18): NARMA-L2 controller at (90 N.m.) load torque (A) Speed response, (B) Torque response.

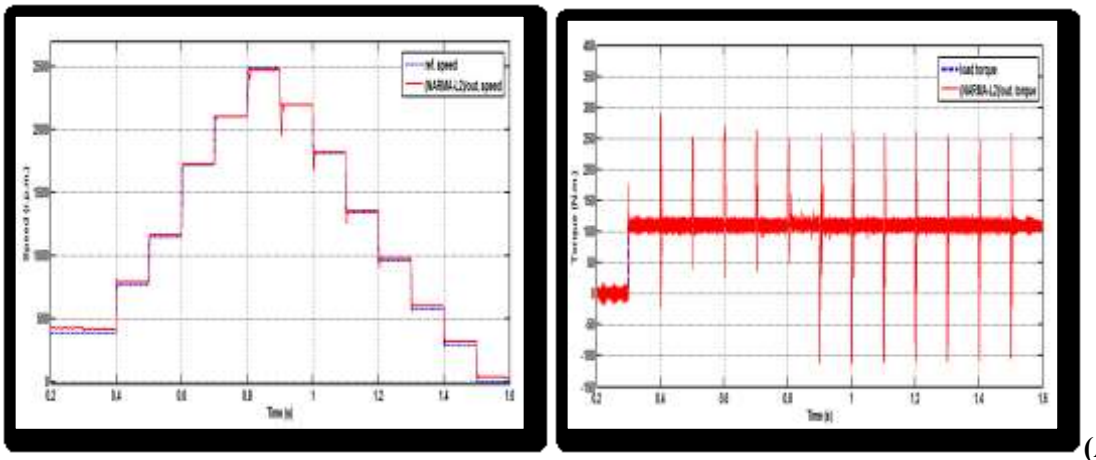

(A)

(B)

Figure (19): NARMA-L2 controller at (110 N.m.) load torque (A) Speed response, (B) Torque response.

The speed error is pointed out in Table (1) for PI-PSO controller while Table (2) for NARMA-L2 controller.

Table (1): The Motor responses of the speed of the DTC of PMSM for PI controller tuning by PSO method at variable speed with variable load torque.

Reference speed in(rad/s)	Reference Speed in (r.p.m.)	Time of calculating speed error in seconds	Error of speed in r.p.m. at no load	Error of speed in r.p.m. at 50 N.m.	Error of speed in r.p.m. at 70 N.m.	Error of speed in r.p.m. at 90 N.m.	Error of speed in r.p.m. at 110 N.m.
40	382	3.5	22	58	93	145	200
80	764	4.5	21	58	87	129	144
120	1146	5.5	16	54	82	106	142
180	1720	6.5	15	50	76	101	123
220	2102	7.5	11	46	69	92	114
260	2484	8.5	12	41	63	83	103
230	2197	9.5	11	38	56	76	96
190	1814	1.05	10	34	52	69	88
140	1338	1.15	11	31	45	61	77
100	955	1.25	11	27	42	55	70
60	573	1.35	10	25	41	55	69
30	287	1.45	9	26	41	55	69
0	0	1.55	10	10	24	28	30

Table (2): The motor responses of the speed of the DTC of PMSM for NARMA-L2 controller at variable speed with variable load torque.

Reference speed in(rad/s)	Reference speed in (r.p.m.)	Time of calculating speed error in seconds	Error of speed in r.p.m. at no load	Error of speed in r.p.m. at 50 N.m.	error of speed in r.p.m. at 70 N.m.	Error of speed in r.p.m. at 90 N.m.	Error of speed in r.p.m. at 110 N.m.
40	382	3.5	38	38	35	33	30
80	764	4.5	36	30	29	26	23
120	1146	5.5	27	23	21	19	18
180	1720	6.5	18	14	12	8	8
220	2102	7.5	10	7	0	0	0
260	2484	8.5	0	0	0	3	5
230	2197	9.5	12	0	3	0	0
190	1814	1.01	18	12	11	9	8
140	1338	1.15	25	20	18	15	14
100	955	1.25	31	27	25	22	21
60	573	1.35	38	34	32	31	29
30	287	1.45	42	38	36	35	33
0	0	1.55	41	38	37	35	33

Table (2) illustrates the error of speed response for NARMA-L2 controller is less than the error PI-PSO controller at the same speed with the different load torque. However, PI controller has less speed error at no load because the PI parameters are tuned at no load condition. Consequently, it is evident that the step response of DTC with NARMA-L2 controller shows improvement in performance and superiority over PI-controller performance with gains tuned by PSO method which eliminates the error in the speed response. This improvement in controller performance obtained is due to the training ability of ANN controller which makes this controller more robust and efficient for wide industrial applications.

The problem of step input is the PMSM may be losing the synchronization. To overcome stepping loss of synchronization the use of ramp input is one of the best solutions. Figure (20) shows the speed response for PI-PSO and NARMA-L2 controllers with load variation in the same operation. Table (3) illustrates the error of speed in this case.

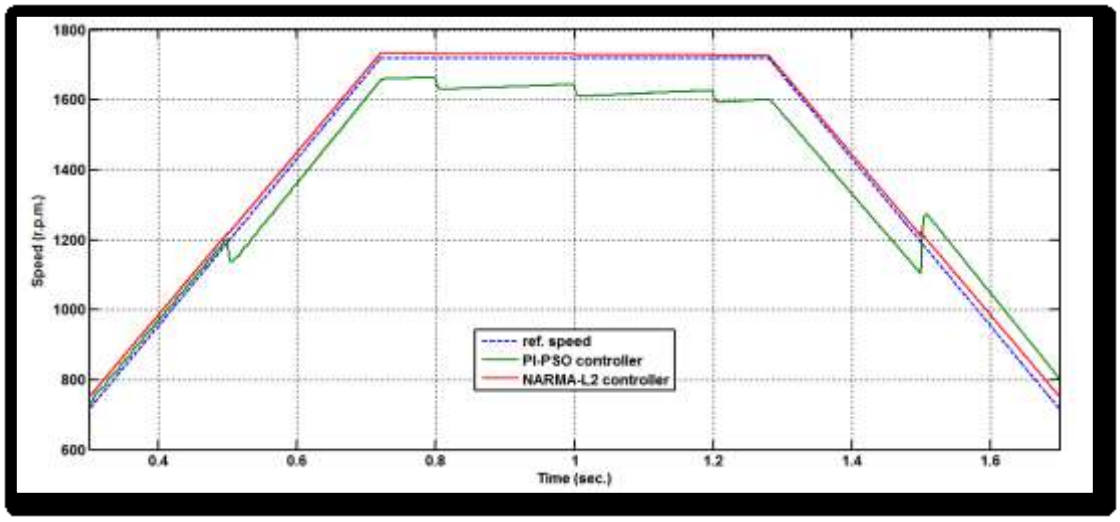

Figure (20): Speed response of (PI-PSO & NARMA-L2 controllers) with load variation.

Table (3): The comparison between (PI-PSO & NARMA-L2 controllers) with load variation and using two ramps input.

	Cases of load torque					
Cases of load torque	**No load, at 0.4 sec, where speed is about (955) r.p.m.**	**(50) N.m., at 0.6 sec, where speed is about (1432) r.p.m.**	**(70) N.m., at 0.9 sec, where speed is about (1720) r.p.m.**	**(90) N.m., at 1.1 sec, where speed is about (1720) r.p.m.**	**(110) N.m., at 1.4 sec, where speed is about (1432) r.p.m.**	**No load, at 1.6 sec, where speed is about (955) r.p.m.**
PI-PSO controller	15	71	83	101	100	95
NARMA-L2 controller	25	18	13	11	14	33

Figure (20) and Table (3) shows the superiority of the NARMA-L2 controller versus PI-PSO controller. NARMA-L2 controller for DTC system of PMSM improves error of speed response making this controller more robust to variation in load than the PI-PSO controller

CONCLUSION

The selection of the PI-controller gains by trial and error is difficult and taken a long time. In order to overcome that difficulty, the PSO is used for optimal gains tuning. PSO tuning skill takes short time and has rapid convergence. This technique creates PI-controller supervisor compared with conventional PI controller with trial and error tuning method due to the improvement in PMSM in terms of less error and more smooth performance of speed compared to conventional PI controller.

NARMA-L2 controller is a robust controller with a good performance due to the training ability of ANN. NARMA-L2 controller shows improvement in performance of DTC and superiority over optimal PI controller for PMSM.

REFERENCES

[1] K. Chikh, M. Khafallah and A. Saad, "Improved DTC Algorithms forReducing Torque and Flux Ripples of PMSM Based on Fuzzy Logic and PWM Techniques", MATLAB- A Fundamental Tool for Scientific Computing and Engineering Applications, Vol. 1, 2012, http://creativecommons/licenses/by/3.0.

[2] D. Ocen, " Direct Torque Control of a Permanent Magnet Synchronous Motor", M.Sc. Thesis, Department of Signals, Sensor and Systems, Royal Institute of Technology (KTH), Stockholm, Sweden, May, 2005.

[3] S. Zhengqiang, H. Zhijian and J. Chuanwen, "Intelligent Control for Permanent Magnet Synchronous Motor with Improved Particle Swarm Optimization", Proceedings of the 5th WSEAS/IASME Int. Conf. on Systems Theory and Scientific Computation, Malta, pp.194-198, September 15-17, 2005.

[4] K. A. Jalal, "Direct Torque Control of Induction Motor Based on Intelligent Systems", Ph.D. Thesis, Department of Electrical and Electronic, University of Technology, Baghdad, Iraq, 2007.

[5] B. Singh, P. Jain, A. P. Mittal and J. R. P. Gupta, "Torque Ripples Minimization of DTC IPMSM Drive for the EV Propulsion System Using a Neural Network", Journal of Power Electronics, Vol. 8, No. 1, January, 2008.

[6] B. Bossoufi, M. Karim, S. Ionita and A. lagrioui, "DTC Control Based Artificial Neural Network for High Performance PMSM Drive", Journal of Theoretical and Applied Information Technology, Vol. 33, No. 2, November 30, 2011.

[7] Dr. Abdulrahim T. Humod & Yasir Thaier Haider, "Study the Robustness of Automatic Voltage Regulator for Synchronous Generator Based on Neuro-Fussy Network", Eng. & Tech. Journal, Vol. 33, Part (A), No. 3, 2015.

[8] Dr. Abdulrahim T. Humod &Wiam I. Jabbar, " Direct Torque Control of an Induction Motor Based on Neurofuzzy", Eng. & Tech. Journal, Vol. 31, Part (A), No.17, 2013.

[9] A. Mishra, J. A. Makwana, P. Agarwal and S. P. Srivastava, "Modeling and Implementation of Vector Control for PM Synchronous Motor Drive", International Conference on Advances in Engineering, Science and Management (ICAESM), IEEE, 978-81-909042-2-3, 2012.

[10] Group PED 4-1031, "Open Loop Low Speed Control for PMSM in High Dynamic Applications", M.Sc. Thesis, Department of Energy Technology, Aalborg University, Denmark, 2010.

[11] J. Singh, B. Singh, S. P. Singh, M. Naim and R. Dixit, "Performance Evaluation of PMSM Drives Using DTC Technique", International Journal of Review in Computing, Vol. 9, April 10, 2012.

[12] A. S. Abdulsada, "Study of AVR Control for Synchronous Generator Based on Intelligent Technique", M.Sc. Thesis, Department of Electrical &Electronic Engineering, University of Technology, Baghdad, Iraq, 2010.

[13] B. Panjwani and V. Mohan, "Comparative Performance Analysis of PID Based NARMA-L2 and ANFIS Control for Continuous Stirred Tank Reactor", International Journal of Soft Computing and Engineering (IJSCE), Vol. 3, Issue 5, November, 2013.

Appendix A

Parameters of permanent magnet 3-phase non-salient pole synchronous motor.

Table (A): Parameters of PMSM from [MATLAB (R2013a) version 8.1 Toolbox].

Item	Value
Rated Power ($\mathbf{P_{out}}$)	39.586 kW
Rated Speed ($\boldsymbol{N}$)	3000 rpm
Rated Torque ($\boldsymbol{T}$)	111 Nm
Continuous Still Torque ($\boldsymbol{T}$)	126 Nm
Number of pole pairs ($\boldsymbol{P}$)	4
Stator Phase Resistance ($\boldsymbol{R_s}$)	1.04 Ω
Armature Inductance ($\mathbf{L_d and L_d}$)	6.335e^{-4} H
Permanent Linkage established by magnets ($\boldsymbol{\Psi}$)	Wb0.192
Moment of Inertia ($\boldsymbol{J}$)	18.89e^{-4}Kg.m^2
Viscous Damping ($\boldsymbol{B}$)	0.011 N.m.s
Static friction ($\boldsymbol{Tf}$)	0 Nm
DC Voltage ($\boldsymbol{V_{dc}}$)	560 V
Voltage Constant ($\boldsymbol{V\_Peak(L-L)/krpm}$)	139.2998
Torque Constant ($\boldsymbol{Nm / A\_peak}$)	1.152

Appendix B

Switching lookup table for DTC of PMSM for inverter by Takashashi and Nouguchi.

Flux error	Torque error	Flux sectors					
		S1	S2	S3	S4	S5	S6
1	1	110	010	011	001	101	100
	0	111	000	111	000	111	000
	-1	101	100	110	010	011	001
0	1	010	011	001	101	100	110
	0	000	111	000	111	000	111
	-1	001	101	100	110	010	011